J|A|C|S
ARTICLES
Published on Web 07/07/2006

Synthetic, Structural, Mechanistic, and Computational Studies on Single-Site β-Diketiminate Tin(II) Initiators for the Polymerization of *rac*-Lactide

Andrew P. Dove, Vernon C. Gibson,* Edward L. Marshall, Henry S. Rzepa, Andrew J. P. White, and David J. Williams

Contribution from the Department of Chemistry, Imperial College London, Exhibition Road, London SW7 2AZ, U.K.

Received March 8, 2006; E-mail: V.Gibson@imperial.ac.uk

Ⓦ This paper contains enhanced objects available on the Internet at http://pubs.acs.org/journals/jacsat.

Abstract: A family of tin(II) complexes supported by β-diketiminate ligands has been investigated as initiators for the polymerization of *rac*-lactide. Kinetic studies reveal a first-order dependence on [lactide], but with a significant induction period. Linear plots of M_n versus conversion and $[M]_o/[I]_o$ versus conversion, along with narrow molecular weight distributions (typically 1.07−1.10), are indicative of well-controlled, "living" polymerizations. Less sterically hindered derivatives promote faster propagation than their bulky analogues, in accord with a more accessible active site. Enhanced rates of polymerization are observed for ligands bearing halogenated *N*-aryl substituents, a consequence of the more Lewis acidic nature of the Sn(II) centers. All of the initiators exhibit a similar bias toward heterotactic polylactide, which is attributed to a chain-end control mechanism influenced predominantly by the presence of the Sn $5s^2$ lone pair of electrons rather than the steric or electronic properties of the β-diketiminate ligand. The tin(II) isopropyl-(*S*)-lactate complex, ($_{Me}BDI_{DIPP}$)SnOCH(Me)COO^{i}Pr (**14**), has been synthesized as a model compound for the propagating species by treatment of ($_{Me}BDI_{DIPP}$)Sn(NMe$_2$) with isopropyl-(*S*)-lactate. An X-ray structure determination showed that the lactate ligand forms a five-membered chelate ring with a weak donor bond from the carbonyl oxygen atom to the tin center. A B3LYP density functional computational study indicates that insertion of the first lactide monomer into the tin(II) alkoxide bond is facile, with the induction period arising from a slower insertion of the second (and possibly third and fourth) monomer units.

Introduction

In recent years, there has been increasing interest in materials derived from biorenewable resources as environmentally sustainable alternatives to petrochemical-derived products. Among the most prominent examples is polylactide (PLA),[1] which is presently being developed as a commodity polymer for packaging, film, and fiber applications. Polylactide and its copolymers, most typically derived from lactide and glycolide, have been employed for many years in speciality biomedical applications,[2] including their use as bioresorbable sutures and orthopedic implants, drug delivery agents, and scaffolds for tissue engineering.

At present, PLA is prepared industrially via the ring-opening polymerization of L-lactide (LA) using tin(II) carboxylate catalysts such as bis(2-ethylhexanoate)tin ($SnOct_2$).[3−7] It is now widely accepted that the active initiator in this catalyst system is a tin(II) alkoxide species generated in situ upon reaction of $SnOct_2$ with alcoholic additives or feedstock impurities.[5,6,8,9] Consistently, bis(alkoxide) complexes such as Sn(OBu^n)$_2$ are active initiators for lactide polymerization.[10,11]

Due to the importance of divalent tin catalysts in the commercial production of polylactide and its copolymers, we decided to investigate the possibility of stabilizing a single-site tin(II) initiator that might polymerize lactide under relatively mild conditions and in a well-controlled fashion in order to facilitate the synthesis of tailored polylactide products. In an earlier communication we showed that a mono-alkoxide tin(II) complex can be synthesized using the sterically demanding *N*,*N*′-bis(2,6-diisopropylphenyl) (DIPP) β-diketiminate ligand (Scheme 1), and we found that this complex polymerized *rac*-LA in a well-controlled manner to give polylactide with a slight het-

(1) Drumright, R. E.; Gruber, P. R.; Henton, D. E. *Adv. Mater.* **2000**, *12*, 1841.
(2) Middleton, J. C.; Tipton, A. J. *Biomaterials* **2000**, *21*, 2335.
(3) Nijenhuis, A. J.; Grijpma, D. W.; Pennings, A. J. *Macromolecules* **1992**, *25*, 6419.
(4) Schwach, G.; Coudane, J.; Engel, R.; Vert, M. *J. Polym. Sci., Part A: Polym. Chem.* **1997**, *35*, 3431.
(5) Kricheldorf, H. R.; Kreiser-Saunders, I.; Boettcher, C. *Polymer* **1995**, *36*, 1253.
(6) Kowalski, A.; Duda, A.; Penczek, S. *Macromolecules* **2000**, *33*, 689.
(7) Kricheldorf, H. R. *Macromol. Symp.* **2000**, *153*, 55.
(8) In't Veld, P. J. A.; Velner, E. M.; van de Witte, P.; Hamhuis, J.; Dijkstra, P.; Feijen J. *J. Polym. Sci. Part A: Polym. Chem.* **1997**, *35*, 219.
(9) Du, Y. J.; Lemstra, P. J.; Nijenhuis, A. J.; van Aert, H. A. M.; Bastiaansen, C. *Macromolecules* **1995**, *28*, 2124.
(10) Kowalski, A.; Libiszowski, J.; Duda, A.; Penczek, S. *Macromolecules* **2000**, *33*, 1964.
(11) Duda, A.; Penczek, S.; Kowalski, A.; Libiszowski, J. *Macromol. Symp.* **2000**, *153*, 41.

10.1021/ja061400a CCC: $33.50

Scheme 1

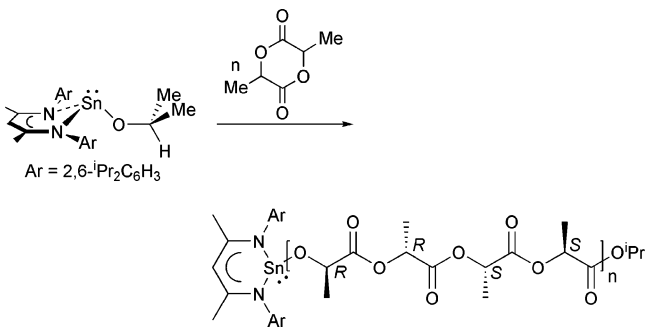

Scheme 2 [a]

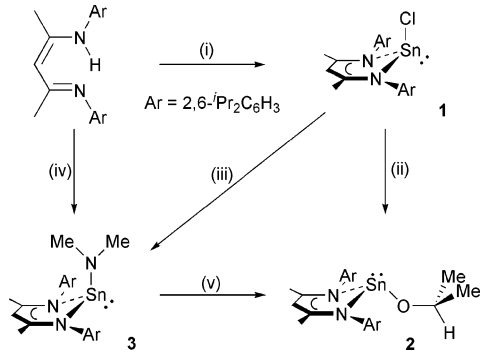

[a] Reagents: (i) ^{n}BuLi, $SnCl_2$; (ii) LiO^iPr; (iii) $LiNMe_2$; (iv) $Sn(NMe_2)_2$; (v) ^{i}PrOH.

erotactic bias.[12] This tin system forms part of a wider family of single-site divalent metal initiators supported by β-diketiminate ligands, including, for example, derivatives based on Zn,[13,14] Mg,[14−17] Fe,[18] and Ca.[19,20] Tolman and co-workers have additionally reported a single-site tin(II) initiator supported by sterically demanding benzamidinate ligands.[21]

Here, we report extensions of our work on divalent tin initiators to a variety of other β-diketiminate ligands of general formula [HC{C(R)═NAr}$_2$] (abbreviated as $_R$BDI$_{Ar}$). We were especially interested in exploring the effect of changes to the steric and electronic properties of the ligand substituents on polymerization rates and molecular weight control, as well as their potential for controlling the tacticity of the polylactide products.

Results

Polymerization of *rac*-Lactide by ($_{Me}$BDI$_{DIPP}$)SnO^{i}Pr. [$_{Me}$BDI$_{DIPP}$]Sn(O^{i}Pr) (**2**, DIPP = 2,6-di-isopropylphenyl) can be prepared by either of the two routes shown in Scheme 2. One involves treatment of [$_{Me}$BDI$_{DIPP}$]Li with $SnCl_2$ to give [$_{Me}$BDI$_{DIPP}$]SnCl (**1**),[12,22] followed by its reaction with LiO^iPr. The second proceeds via the reaction of [$_{Me}$BDI$_{DIPP}$]H with Sn(NMe$_2$)$_2$[23] to afford [$_{Me}$BDI$_{DIPP}$]Sn(NMe$_2$) (**3**), followed by its alcoholysis with 1 equiv of ^{i}PrOH.

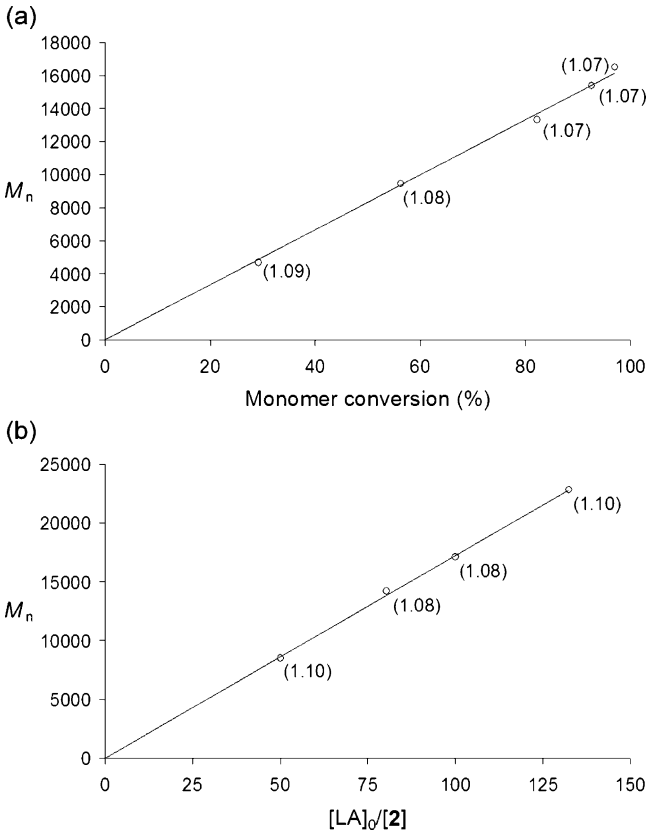

Figure 1. (a) Plot of M_n vs monomer conversion for the polymerization of *rac*-LA initiated by complex **2** (25 °C, CH_2Cl_2, $[LA]_0/[2] = 100$) (b) Plot of M_n vs $[LA]_0/[2]$ (60 °C, toluene); polydispersities are given in parentheses. M_n was determined by GPC in $CHCl_3$ vs polystyrene calibrants (see Supporting Information).

Complex **2** polymerizes *rac*-LA slowly at room temperature, requiring 50 h to attain >95% conversion of 100 monomer equivalents. The polymerization is well-controlled, producing PLA with an M_n value close to that predicted from the monomer-to-initiator ratio [M_n(obs) = 17 100 Da, M_n(calc) = 14 400 Da] and a very narrow molecular weight distribution (M_w/M_n = 1.05). In accord with a well-behaved chain propagation process, M_n increases linearly with monomer conversion, and low M_w/M_n values are maintained throughout the polymerization (Figure 1a). NMR spectroscopic analysis reveals a small bias toward a heterotactic assembly,[12] with notably increased concentrations of the *rmr* and *mrm* tetrads[24] compared to those predicted by Bernoullian statistics for a random, atactic assembly.[25] At 60 °C in toluene, the polymerization proceeds to >90% monomer conversion within 4 h. M_n and M_w/M_n values are comparable to those obtained at ambient temperature (M_n = 17 100 Da, M_w/M_n = 1.08), with M_n again exhibiting a linear correlation with monomer conversion and monomer-to-initiator stoichiometry (Figure 1b).

The propagation process can be conveniently followed by ^{1}H NMR spectroscopy at room temperature; selected spectra of a 1:10 mixture of [**2**]:[LA] in $CDCl_3$, recorded over a period

(12) Dove, A. P.; Gibson, V. C.; Marshall, E. L.; White, A. J. P.; Williams, D. J. *Chem. Commun.* **2001**, 283.
(13) Cheng, M.; Attygalle, A. B.; Lobkovsky, E. B.; Coates, G. W. *J. Am. Chem. Soc.* **1999**, *121*, 11583.
(14) Chamberlain, B. M.; Cheng, M.; Moore, D. R.; Ovitt, T. M.; Lobkovsky, E. B.; Coates, G. W. *J. Am. Chem. Soc.* **2001**, *123*, 3229.
(15) Chisholm, M. H.; Huffman, J. C.; Phomphrai, K. *Dalton Trans.* **2001**, 222.
(16) Chisholm, M. H.; Gallucci, J.; Phomphrai, K. *Inorg. Chem.* **2002**, *41*, 2785.
(17) Gibson, V. C.; Marshall, E. L.; Dove, A. P. Patent WO 0238574.
(18) Gibson, V. C.; Marshall, E. L.; Navarro-Llobet, D.; White, A. J. P.; Williams, D. J. *Dalton Trans.* **2002**, 4321.
(19) Chisholm, M. H.; Gallucci, J.; Phomphrai, K. *Chem. Commun.* **2003**, 48.
(20) Chisholm, M. H.; Gallucci, J.; Phomphrai, K. *Inorg. Chem.* **2004**, *43*, 6717−6725.
(21) Aubrecht, K. B.; Hillmyer, M. A.; Tolman, W. B. *Macromolecules* **2002**, *35*, 644−650.
(22) Stender, M.; Wright, R. J.; Eichler, B. E.; Prust, J.; Olmstead, M. M.; Roesky, H. W.; Power, P. P. *Dalton Trans.* **2001**, 3465.
(23) Foley, P.; Zeldin, M. *Inorg. Chem.* **1975**, *14*, 2264.

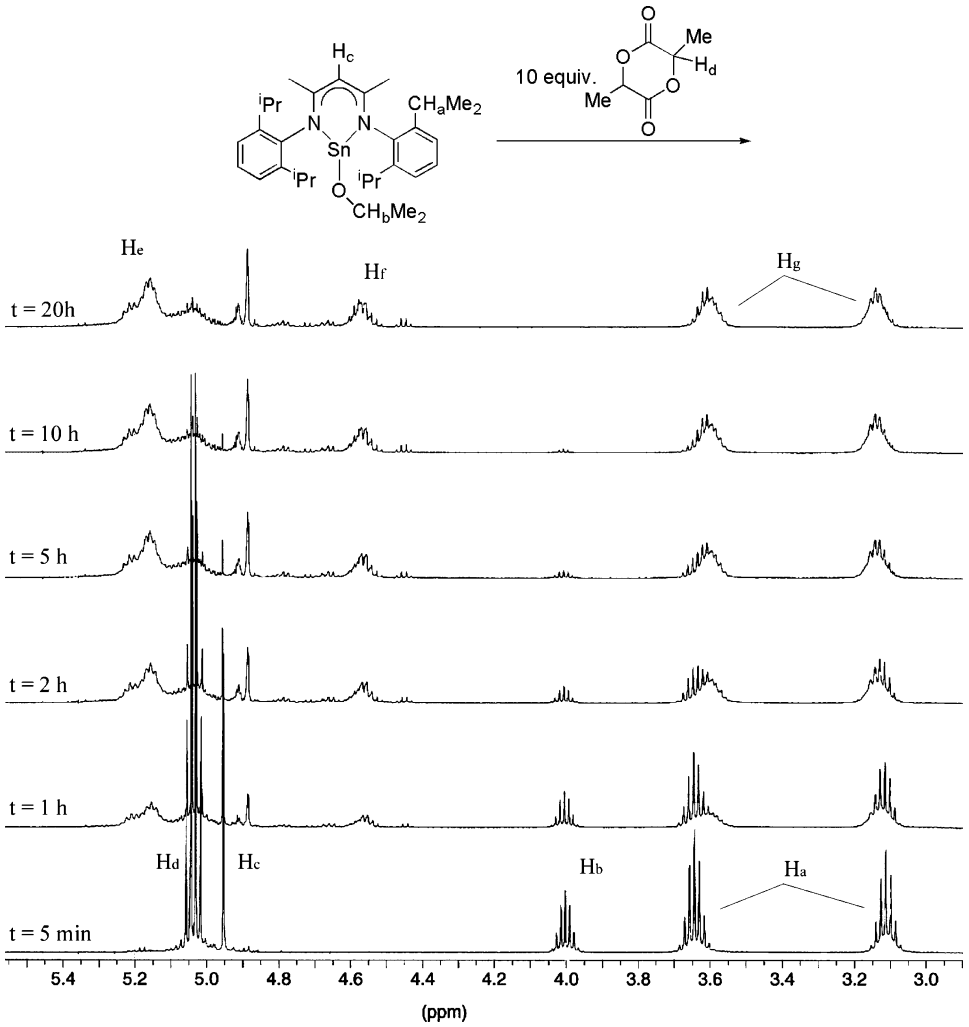

Figure 2. 250 MHz ^{1}H NMR spectra (δ 2.9−5.5) for the reaction of complex **2** with *rac*-LA (25 °C, $CDCl_3$, $[LA]_0/[\mathbf{1}] = 10$); see text for assignments of H_{e-g}.

of 20 h, are shown in Figure 2. Initially, resonances are observed for **2** (aryl CH_aMe$_2$ methine septets at δ 3.10 and δ 3.65, the OCH_bMe$_2$ septet at δ 4.00, and a singlet at δ 4.95, due to the methine group in the β-diketiminate backbone, H_c) and for unconsumed monomer (the methine H_d resonance visible as a quartet at δ 5.05). As the polymerization commences, these resonances diminish in intensity and are replaced by signals attributable to propagating species. These include a broad signal at δ 5.2, H_e, due to the methine resonance of propagating PLA oligomers and a multiplet at δ 4.55, H_f, corresponding to a $CO_2{}^i$Pr ester end-group; the corresponding doublet resonances are observed at δ 0.95 and δ 0.87, respectively. The observation of ester chain termini implies that ring-opening of the cyclic ester monomer occurs via cleavage of an acyl−oxygen bond, as found for other metal alkoxide initiating systems.[26−33] The other notable feature of the spectra is the gradual broadening of the β-diketiminate aryl CHMe$_2$ resonances as H_a is replaced by H_g; such broadening is consistent with the formation of propagating chains differing only in chain length and/or tacticity.

A linear correlation between $\ln\{[LA]_t/[LA]_0\}$ and reaction time indicates that propagation is first order in monomer concentration. Similar analyses over a range of initiator concentrations (Figure 3a) afforded a plot of $\ln k_{app}$ against $\ln$ [**2**] from which the order in initiator was found to be 1.10 ± 0.04 (Figure 3b). It is clear from Figure 3a that the plots would not extrapolate through the origin and that there is an apparent induction period of ∼42 min at 60 °C. Thereafter, propagation proceeds with an apparent rate constant, k_{app}, of 0.736 ± 0.049 h^{-1}. We shall return to examine the nature of this induction period in more detail.

Synthesis and Characterization of Related β-Diketiminate Tin(II) Initiators. The synthetic pathways outlined in Scheme 2 have been used to synthesize derivatives containing a range of β-diketiminate ligands of general formula [HC{C(R)═NAr}$_2$]; these are summarized in Figure 4.

In addition to complexes **1**−**3**, which contain methyl substituents on the ligand backbone, the chloride and isopropoxide

(24) The *m*/*r* (*m* = meso; *r* = racemic) notation is an alternative to the *i*/*s* (*i* = iso; *s* = syndio) system also encountered in the literature.
(25) Kricheldorf, H. R.; Boettcher, C.; Tönnes, K. U. *Polymer* **1992**, *33*, 2817.
(26) Trofimoff, L.; Aida, T.; Inoue, S. *Chem. Lett.* **1987**, 991.
(27) Shimasaki, K.; Aida, T.; Inoue, S. *Macromolecules* **1987**, *20*, 3076.
(28) Kricheldorf, H. R.; Berl, M.; Scharnagl, N. *Macromolecules* **1988**, *21*, 286.
(29) Dubois, Ph.; Jacobs, C.; Jérôme, R.; Teyssié, Ph. *Macromolecules* **1991**, *24*, 2266.
(30) Stevels, W. M.; Ankoné, M. J. K.; Dijkstra, P. J.; Feijen, J. *Macromol. Chem. Phys.* **1995**, *196*, 1153.
(31) Chisholm, M. H.; Eilerts, N. W. *Chem. Commun.* **1996**, 853.
(32) LeBorgne, A.; Pluta, C.; Spassky, N. *Macromol. Rapid Commun.* **1994**, *15*, 955.
(33) Ihara, E.; Tanabe, M.; Nakayama, Y.; Nakamura, A.; Yasuda, H. *Macromol. Chem. Phys.* **1999**, *200*, 758.

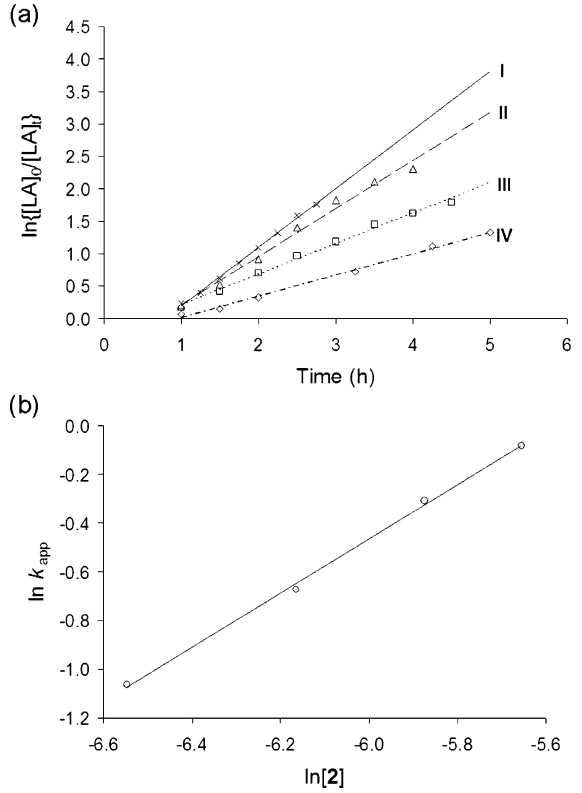

Figure 3. (a) Semilogarithmic plots of *rac*-LA conversion with time initiated by complex **2** (60 °C, toluene, $[LA]_0 = 0.28$ M; for **I**, $[2] = 0.0035$ M; for **II**, $[2] = 0.0028$ M; for **III**, $[2] = 0.0021$ M; for **IV**, $[2] = 0.0014$ M). (b) Plot of ln k_{app} vs ln [**2**] for the polymerization of *rac*-LA initiated by **2** (60 °C, toluene).

derivatives **4** and **5**, bearing *tert*-butyl backbone substituents, have been prepared. The effect of the *tert*-butyl substituents is to force the N-aryl groups to project further forward, effectively increasing steric hindrance around the active site.[34,35] Lithiation of $[_{tBu}BDI_{DIPP}]H$, followed by addition to $SnCl_2$, afforded $[_{tBu}BDI_{DIPP}]SnCl$ (**4**) in good yield (ca. 80%). The reaction required heating at 80 °C for 18 h, compared to 25 °C for the analogous synthesis of **1**, reflecting the increased steric hindrance of the *tert*-butyl-substituted diketimine. Addition of 1.0 equiv of LiO^iPr to **4**, followed by stirring at 80 °C for 18 h, gave **5** in ca. 70% yield.

The less sterically crowded tin(II) alkoxides $[_{Me}BDI_{DMP}]SnO^iPr$ (**7**, DMP = 2,6-dimethylphenyl) and $[_{Me}BDI_{Ph}]SnO^iPr$ (**9**) have been prepared in an analogous manner via the addition of LiO^iPr to the appropriate chloride complexes **6** and **8**, respectively. Although the synthesis of complex **7** proceeded in high yield, **9** was initially isolated as an impure oily solid. Purification was achieved by repeated washing with cold heptane, but yields are consequently lowered (to ca. 20%). Due to the problems associated with the synthesis of **9** via this route, the corresponding amide, $[_{Me}BDI_{Ph}]SnNMe_2$ (**10**), was synthesized by the addition of $[_{Me}BDI_{Ph}]H$ to $Sn(NMe_2)_2$ in toluene (67%). However, attempts to convert **10** into **9** via treatment with ^iPrOH resulted in unclean product mixtures.

The amide derivatives **11**−**13**, containing electron-withdrawing halo substituents, were similarly prepared in a straightforward manner by addition of the β-diketimines $[_{Me}BDI_{DCP}]H$, $[_{Me}BDI_{TCP}]H$, and $[_{Me}BDI_{TBP}]H$, respectively, to $Sn(NMe_2)_2$ (DCP = 2,6-dichlorophenyl; TCP = 2,4,6-trichlorophenyl; TBP = 2,4,6-tribromophenyl).

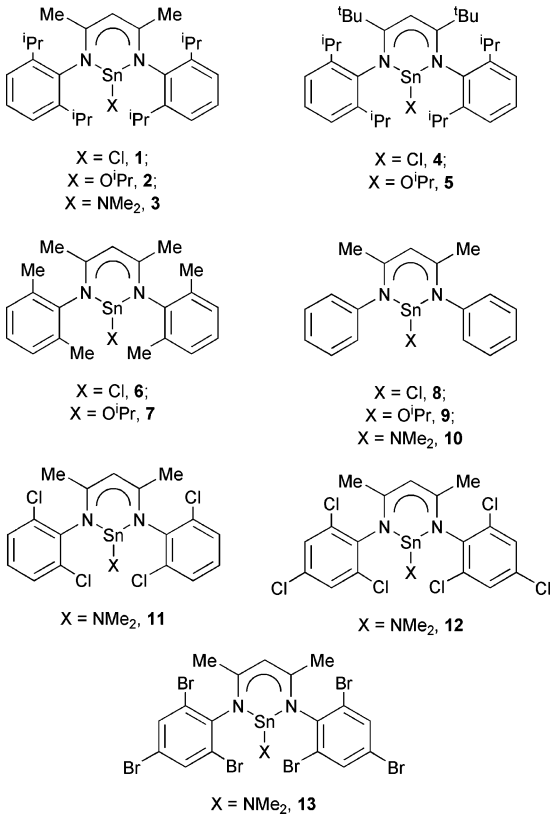

Figure 4. $(RBDI_{Ar})SnX$ complexes synthesized in this study.

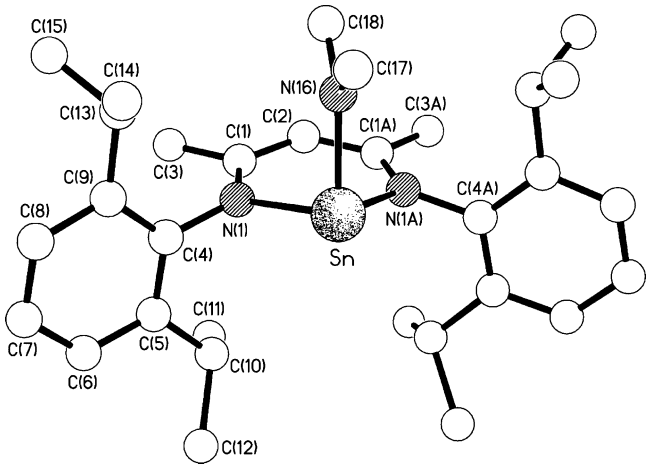

Figure 5. Molecular structure of complex **3**. The N(1)−Sn−N(16) angle is 95.59(12)°; other relevant bond lengths and angles are given in Table S1.

X-ray Crystallography. X-ray-quality crystals of complexes **3**, **9**, and **12** were grown and analyzed as described in the Supporting Information. Their molecular structures (Figures 5−7) all show the tin centers to adopt a trigonal pyramidal geometry with angles of 90−100° between the nitrogen donors of the β-diketiminate ligands and the oxygen or nitrogen donor atoms of the ancillary alkoxide or amide ligands, respectively. This geometrical constraint arises from the effect of a relativistic contraction of the tin 5s orbital, resulting in only a small amount of mixing with other tin-based orbitals. Thus, the bonding is

(34) Budzelaar, P. H. M.; van Oort, A. B.; Orpen, A. G. *Eur. J. Inorg. Chem.* **1998**, 1485.
(35) Bailey, P. J.; Coxall, R. A.; Dick, C. M.; Fabre, S.; Parsons, S. *Organometallics* **2001**, *20*, 798.

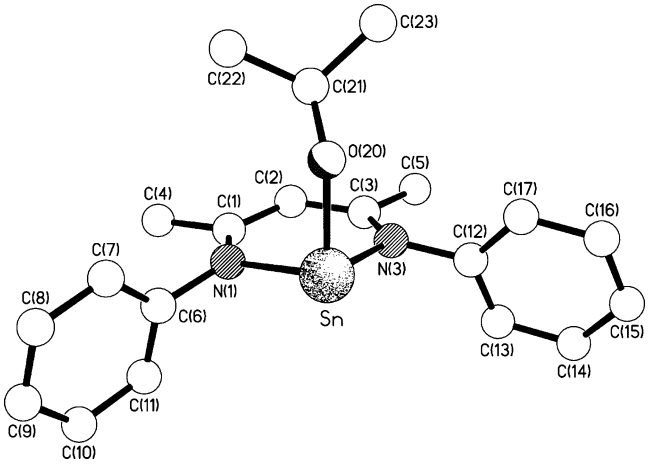

Figure 6. Molecular structure of complex **9**. Selected bond angles (°): N(1)−Sn−O(20) = 98.2(4), N(3)−Sn−O(20) = 93.8(3).

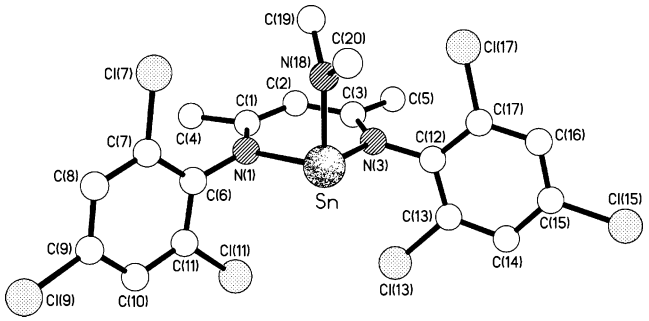

Figure 7. Molecular structure of complex **12**. Selected bond angles (°): N(1)−Sn−N(18) = 95.8(2), N(3)−Sn−N(18) = 96.1(2).

dominated by interactions of the ligand donor atoms with the tin p and d orbitals; the lone pair remains nonbonding and occupies quite a large and diffuse region of space.

For complex **3** (Figure 5), the two 2,6-diisopropylphenyl rings are oriented orthogonally (ca. 90°) to the {N(1),C(1),C(1A), N(1A)} plane, a conformation that is possibly stabilized by pairs of C−H···N(pπ) interactions between the isopropyl methine protons and the nitrogen center [H···N = 2.47 and 2.57 Å].[36] There are no significant intermolecular interactions, the closest approach to the phenyl ring being 3.19 Å from an isopropyl methyl proton. In complex **9**, the isopropoxide ligand is folded back over the six-membered chelate ring (Figure 6), but any potential interaction between the isopropyl methine proton and the six-membered chelate ring is discounted on the basis of the proton lying ca. 2.59 Å away from the {N1,C1,C3,N3} plane, with a noticeably enlarged Sn−O(20)−C(21) angle of 129.8-(8)°. The two phenyl rings, which are both less steeply inclined to the {N1,C1,C3,N3} plane than in complex **3** (ca. 70°), are involved in a series of weak intermolecular C−H···π interactions. The C(6) phenyl ring in one molecule is approached from opposite sides by C(13)−H [H···π = 2.78 Å, C−H···π = 157°] and C(22)−H [H···π = 2.82 Å, C−H···π = 154°] from two symmetry-related molecules, the two interactions subtending an angle of ca. 160° at the C(6)−ring centroid. The C(12) phenyl ring is approached by the C(8)−H proton in another molecule (H···π = 2.82 Å, C−H···π = 148°). The closest approach to the O(20) oxygen atom is from the C(2)−H proton of a lattice-translated (along *a*) counterpart at C···O = 3.39 Å, H···O = 2.51 Å, C−H···O = 153°. The two pendant aromatic rings in complex **12** (Figure 7) are oriented virtually orthogonally (ca. 93°) to the {N1,C1,C3,N3} plane, and adjacent lattice-translated (along *b*) molecules are linked by a weak C−H···π interaction between the C(8)−H proton and the C(12) phenyl ring, with H···π = 2.89 Å and C−H···π = 132°. Further discussion of other aspects of the structures of **3**, **9**, and **12**, including a comparison with related molecules, can be found in the Supporting Information.

Table 1. Data for the Polymerization of *rac*-LA Using Tin(II) Alkoxide and Amide Complexes[a]

initiator	time (h)[b]	conv (%)[c]	k_{app} (h^{-1})	induction period (min)[d]	M_n (Da)[e]	M_w/M_n[e]	P_r[f]
2	4	94	0.736 ± 0.049	42	17 100	1.06	0.64
3	7	92	0.703 ± 0.043	150	17 000	1.18	0.64
5	8	96	0.384 ± 0.020	67	16 000	1.16	0.63
7	3	92	0.996 ± 0.024	24	16 800	1.12	0.65
9	2	93	1.634 ± 0.024	8	17 100	1.13	0.67
10	2.25	93	1.403 ± 0.157	11	17 600	1.18	0.67
11	1.75	92	1.578 ± 0.024	10	19 500	1.23	0.64
12	1.5	91	1.884 ± 0.177	8	21 000	1.19	0.62
13	2.25	91	1.214 ± 0.095	12	20 300	1.24	0.64

[a] Polymerizations performed in toluene at 60 °C; [LA]/[initiator] = 100; [LA] = 2.8 M. [b] Time required for monomer conversion >90%. [c] Conversion, as determined by ^{1}H NMR spectroscopy ($CDCl_3$). [d] Determined by extrapolation of kinetic data. [e] Determined by GPC (vs polystyrene standards $CHCl_3$). [f] Probability of racemic enchainment, as determined by homonuclear decoupled ^{1}H NMR.[13]

Polymerization Studies. The polymerization of *rac*-LA using the alkoxides and amides described above is summarized in Table 1. For the amide initiator **3**, at first sight propagation appears to be slower than for **2**, with high conversions (>90%) being achieved only after 7 h. However, on close examination, a significant part of this (150 min) was found to be due to an induction period and, once initiation had occurred, the apparent rates of propagation for **2** and **3** are similar within experimental error (k_{app}(**2**) = 0.736 ± 0.049 h^{-1}; k_{app}(**3**) = 0.703 ± 0.043 h^{-1}). The polymerization of *rac*-LA using **3** was still well-controlled, with a linear dependence of M_n upon monomer conversion, but the polydispersity was slightly higher than that measured using its isopropoxide counterpart, which is attributable to less efficient initiation by the more sterically hindered NMe_2 derivative (the presence of the CO_2NMe_2 chain end was confirmed by ^{1}H NMR spectroscopy; see Figure 12). The polylactide produced using **3** displayed a microstructure identical to that of the polylactide produced using **2**.

The increased steric influence of the BDI ligand in **5** resulted in a significant slowing of polymerization rate and an increase in the induction period. The observed rate of propagation, k_{app} = 0.384 ± 0.020 h^{-1}, was approximately half that observed for **2**. Although the polymerization was slower, the polymer microstructure remained unchanged.

A decrease in the size of the ortho substituents (cf. **7**, **9**, and **10)** led to an increase in polymerization rate and a decrease in induction period. Hence, **7** consumed >90% monomer within 3 h, with an induction period around half of that observed using **2**. Even faster propagation and a shorter induction period were observed for complexes **9** and **10**. Interestingly, even with sterically less hindered ligands, the tacticities of the polylactide samples produced using **7**, **9**, and **10** are virtually identical to those observed using complexes **2**, **3**, and **5**.

(36) Dove, A. P.; Gibson, V. C.; Hormnirun, P.; Marshall, E. L.; Segal, J. A.; White, A. J. P.; Williams, D. J. *Dalton Trans.* **2003**, 3088.

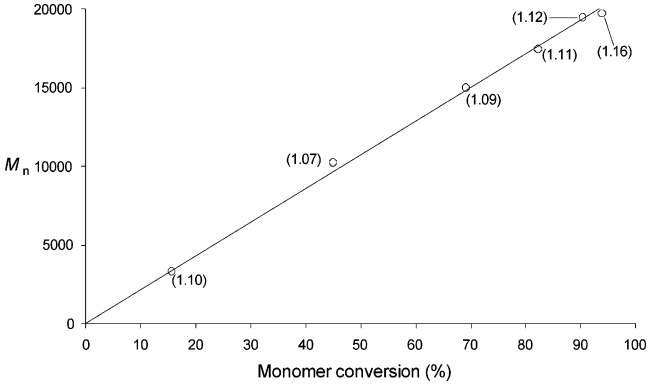

Figure 8. Plot of M_n vs monomer conversion for the polymerization of *rac*-LA initiated by complex **12** (60 °C, toluene, $[LA]_0/[\mathbf{12}] = 100$; polydispersities in parentheses).

Scheme 3. Synthesis of the Sn(II) Lactate Complex, **14**

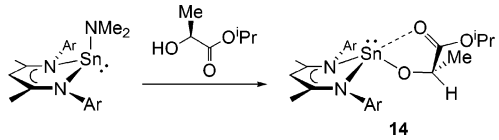

14

The rate of propagation increases when electron-withdrawing halo-substituted β-diketiminate ligands are used. A comparison of the sterically similar *N*,*N*′-bis(2,6-dimethylphenyl) and *N*,*N*′-bis(2,6-dichlorophenyl) derivatives, **7** and **11**, shows a substantial increase in the rate of propagation for the halogenated derivative. Furthermore, the induction period using the amide complex **11** was less than half of that observed using the alkoxide **7**, despite the presence in the former of the more bulky amide nucleophile. The polymerization rate is further enhanced for the 2,4,6-trichloro derivative, **12**, whereas the lower electronegativity of the 2,4,6-tribromo-substituted analogue **13** (and possibly its increased size) afforded a slightly slower polymerization. In all cases, the microstucture of the PLA showed no discernible variation from the slight heterotactic bias observed using **2**.

Although M_n was found to increase linearly with conversion for all three halo-substituted initiators (see, for example, Figure 8), the molecular weights of the isolated polymers derived from **11**−**13** were slightly higher than those prepared from their non-halogenated counterparts. Broader molecular weight distributions were also observed. This is most likely due, in part, to the use of the NMe_2 initiating group which, due to its larger size, initiates less efficiently than O^{i}Pr (cf. **2** and **3**, or **9** and **10**, Table 1). However, low levels of trans-esterification of the PLA chains due to the increased reactivity of the more electron-deficient metal center may also be responsible. An indication that trans-esterification does occur is evident in the broadening of M_w/M_n as the polymerization approached high levels of monomer conversion (Figure 8).

Spectroscopic and Structural Characterization, and Polymerization Behavior, of a Tin(II) Lactate Intermediate. To obtain a better understanding of the propagating species, the complex $[_{Me}BDI_{DIPP}]SnOCH(Me)CO_2{}^iPr$ (**14**) was synthesized by treatment of **3** with isopropyl-(*S*)-lactate (Scheme 3). Crystals of **14** suitable for X-ray diffraction were grown from heptane at −10 °C. The coordination geometry may be viewed (Figure 9a) as being derived from a trigonal bipyramid with a vacant equatorial coordination site. The BDI ligand spans the

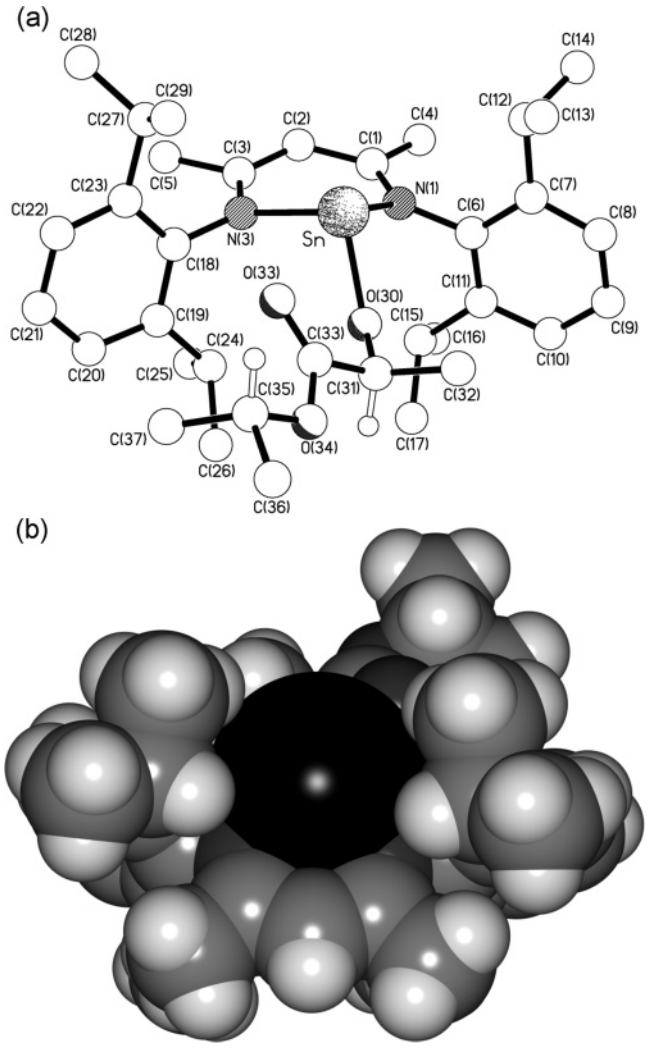

Figure 9. (a) Molecular structure of complex **14**. Selected bond lengths (Å): N(1)−Sn = 2.228(6); N(3)−Sn = 2.223(5); O(30)−Sn = 2.028(6); O(33)−Sn = 2.755(6). Selected bond angles (°): N(1)−Sn−N(3) = 83.1-(2); N(1)−Sn−O(30) = 84.4(3); N(3)−Sn−O(30) = 95.3(2); Sn−O(30)−C(31) = 122.0(5). (b) Space-filling representation showing the exposed tin center.

equatorial and axial sites, while the Sn−O bond of the alkoxo unit occupies an equatorial site. The carbonyl group of the lactate ligand forms only a weak interaction (2.755(6) Å) to the tin by binding in the remaining axial site, trans to N(1) of the BDI ligand. The chelate ring has an asymmetric boat conformation, with the metal atom and C(2) being displaced by 0.87 and 0.13 Å, respectively, out of the {N(1),C(1),C(3),N3} plane, whose atoms are coplanar to within 0.01 Å. The two 2,6-diisopropylphenyl rings are oriented approximately orthogonally to the plane of the chelate ring, the torsional twists about the N(1)−C(6) and N(3)−C(18) bonds being ca. 85 and 83°, respectively. As was observed in the structure of **2**, the O-donor ligand is directed away from the chelate ring, in contrast to the observation in the structure of the related (trifluoromethanesulfonato-O)tin(II) complex, where the sulfonato ligand is folded back to lie over the plane of the chelate ring.[36] The trigonal pyramidal geometry at tin therefore places the metal atom in an exposed position on the surface of the molecule (Figure 9b). There are, however, no close intermolecular approaches to the metal center, the nearest contacts being from the isopropyl group of the lactate ligand in symmetry-related molecules.

Scheme 4. General Reaction Coordinate for the Ring-Opening Polymerization of Lactide[a]

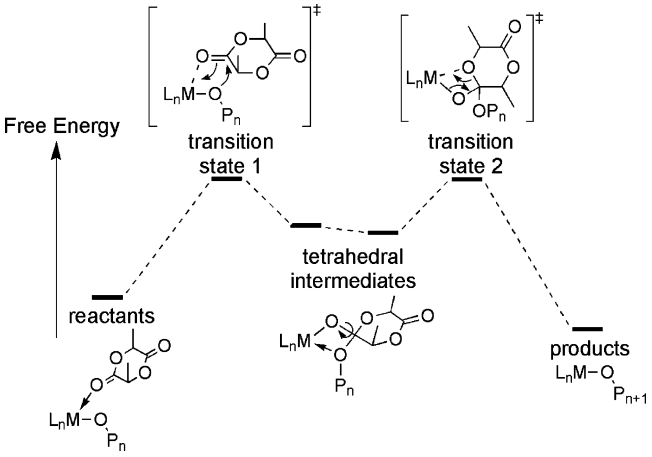

[a] P_n = propagating polyester chain.

The remarkably long metal−carbonyl oxygen interaction in complex **14** contrasts the chelating role played by the lactate ligand in the structure of the related zinc complex *rac*-[$_{Me}$BDI$_{DIPP}$]Zn(μ^2-OCH(Me)CO$_2$Me) (Zn−O$_{carbonyl}$ = 2.189(2) Å)[14] but does still lie within the sum of tin and oxygen van der Waals radii (2.17 + 1.52 = 3.69 Å).[37]

To probe the coordination of the lactate ligand in solution, ^{1}H NOESY and COSY NMR spectra were recorded.[38] These show that the methine proton of the [Sn−OC*H*Me] lactate fragment closely approaches two of the aryl−^{i}Pr substituents. However, the lactate methyl C(32) shows no interactions with any of the β-diketiminate substituents, suggesting that rotation about the Sn−O(30) and the O(30)−C(31) vectors does not readily occur. The low symmetry of complex **14**, arising from the locked nature of the lactate ligand, results in a room-temperature ^{1}H NMR spectrum which includes four septets and eight doublets, arising from the inequivalent ^{i}Pr groups of the β-diketiminate fragment, and two [HC(C(C*H*$_3$)NAr)$_2$] methyl resonances. Although these data are consistent with coordination of the C(33)−O(33) carbonyl to the tin center, the hindered rotation may simply arise as a result of steric congestion around the metal. Evidence for weak coordination of O(33) to the metal in the solution state is provided by a ^{119}Sn NMR chemical shift of −265.3 ppm. Four-coordinate Sn^{II} chemical shifts generally occur in the range δ −550 to δ −650,[39] but the value for **14** is nonetheless larger than the chemical shifts of a wide range of three-coordinate (BDI)SnX complexes (e.g. δ −189.1 for **2**),[38] an observation consistent with weak coordination of the carbonyl group.

A study into the polymerization of *rac*-LA initiated by **14** gave an apparent rate of propagation comparable to that observed using **2** (k_{app}(**14**) = 0.744 ± 0.072 h^{-1}). The molecular weight control is also almost identical (M_n = 15 600, M_w/M_n < 1.10), M_n values again increasing linearly with monomer conversion and the PLA produced showing a comparable heterotactic bias. However, somewhat surprisingly, **14** still afforded an induction period — of approximately 20 min (cf. 42 min for **2**) — before onset of polymerization. Thus, it is clear that **14** is an imperfect model for the propagating species. To understand why this should be so, and to gain more insight into the origin of the induction period, we embarked upon a quantum chemical study.

Scheme 5 [a]

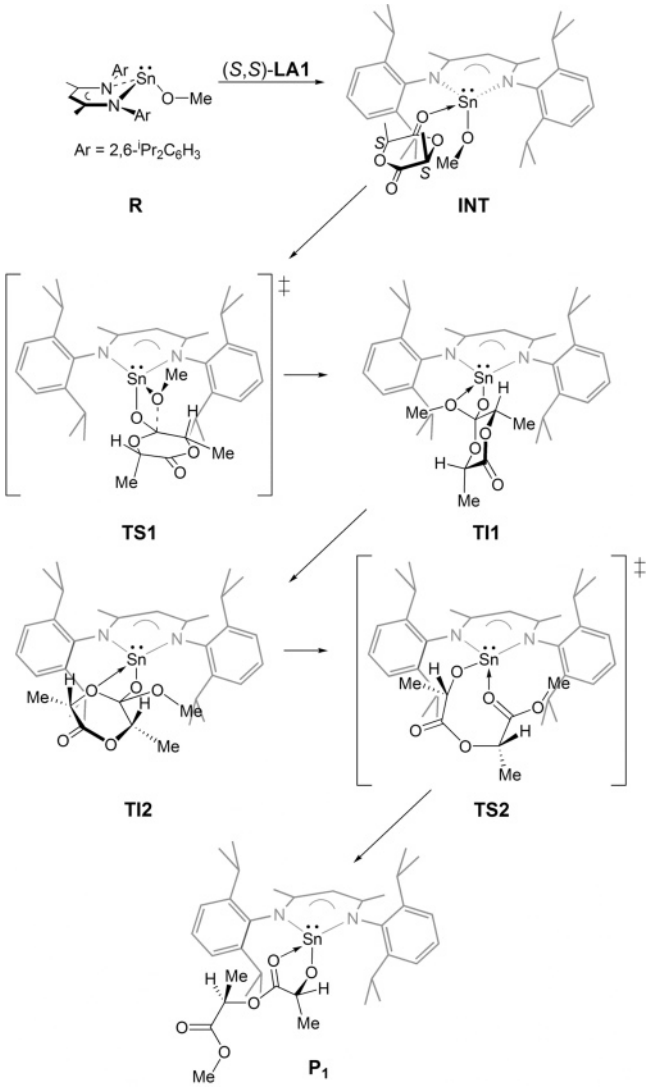

[a] **R**, reactants; **INT**, monomer-bound intermediate, R·LA; **TI**, tetrahedral intermediate; **TS**, transition state; **P**, propagating species. The lone pair is included in the illustrations of intermediates and transition states, not to imply a specific coordination site for the lone pair but to remind the reader that the geometry of the complex is strongly influenced by its presence.

Computational Studies. Recently, we reported a theoretical investigation into the ring-opening polymerization of *rac*-lactide by β-diketiminate magnesium complexes.[40] A schematic of the computed reaction coordinate, which was found to contain two energetically comparable transition states, is shown in Scheme 4. A similar B3-LYP density functional procedure has been carried out on the *N*,*N*′-bis(2,6-diisopropylphenyl) β-diketiminate tin(II) system with one key difference. To address the origin of the induction period, the addition of an (*S*,*S*)-lactide monomer to the tin(II) alkoxide initiator was first examined, followed by insertion of a second (*R*,*R*)-monomer unit into the propagating polyester chain.

(37) Bondi, A. *J. Phys. Chem.* **1964**, *68*, 441.
(38) See Supporting Information.
(39) Harris, R. K.; Mann, B. E. *NMR and the Periodic Table*; Academic Press: London, 1978; pp 342−366.
(40) Marshall, E. L.; Gibson, V. C.; Rzepa, H. S. *J. Am. Chem. Soc.* **2005**, *127*, 6048.

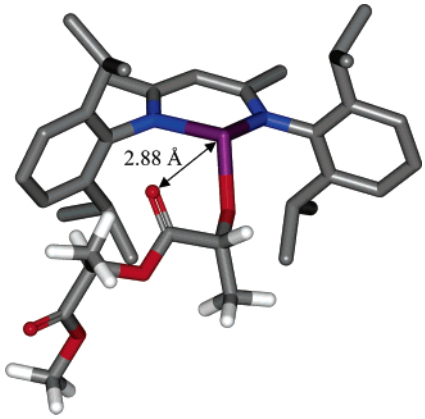

Figure 10. Computed geometry of $\mathbf{P_1}$ (gray, carbon; blue, nitrogen; red, oxygen; purple, tin).

Scheme 6

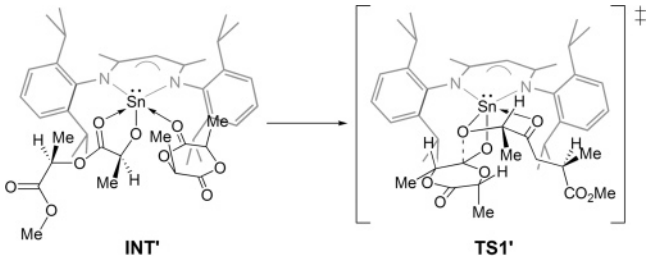

For the reaction between [$_{Me}$BDI$_{DIPP}$]SnOMe and (*S*,*S*)-lactide, the monomer approach is found to be strongly affected by the geometric constraints imposed by the tin lone pair. The monomer initially binds weakly to a site trans to a nitrogen donor of the BDI ligand (**INT**, Scheme 5). To proceed to **TS1**, the first of the two major transition states, the monomer and the alkoxide ligand first exchange sites via a turnstile rotation. The tetrahedral intermediate thus generated (**TI1**) exhibits a Sn···OMe interaction of 3.23 Å, a distance comparable to the long Sn−O$_{carbonyl}$ interaction observed in the molecular structure of **14**. Rotation around the O$_{alkoxide}$−C vector next affords **TI2**, allowing the O$_{acyl}$ atom to approach the tin in readiness for ring-opening (Sn···O$_{acyl}$ = 2.93 Å). Cleavage of the six-membered heterocycle then occurs on passing through **TS2**, comprising an eight-membered ring with a Sn−O$_{alkoxide}$ bond (2.31 Å) and a longer Sn−O$_{carbonyl}$ donor interaction (2.44 Å). Extrusion of the PLA chain from the tin coordination sphere occurs by dissociation of the carbonyl donor interaction and migration of the Sn−alkoxide bond to a resting coordination site similar to the starting complex (**R**). The resting state of the first insertion product, $\mathbf{P_1}$, contains a five-membered Sn lactate, with a long Sn···O$_{carbonyl}$ interaction of 2.88 Å, a value close to that found in complex **14** (2.755(6) Å). The energy-minimized structure of $\mathbf{P_1}$ is shown in Figure 10.

The second insertion follows a similar pattern, but the incoming monomer molecule must now make its approach to the five-membered Sn lactate of $\mathbf{P_1}$, rather than the simple methoxide ligand of **R**. Monomer binds in an analogous site trans to one of the nitrogen donors (**INT′**, Scheme 6), and a turnstile-like rotation is again required in order to position the monomer for attack by the alkoxide (**TS1′**). The gross features of the subsequent steps are similar to those described above for the insertion of the first monomer unit (full details are provided in the Supporting Information).

The free energies for the key steps of both first and second monomer insertions are summarized in Figure 11 (values are shown relative to **R** = 0 kcal mol^{-1}). A number of differences are apparent for the two insertion steps: (i) **TS1** is rate-determining in the initiation step, whereas **TS1′** and **TS2′** have nearly identical free energies for insertion of the second monomer; (ii) intermediates **TI1** and, to a lesser extent, **TI2** are relatively low-lying (1.5 and 5.9 kcal mol^{-1}, respectively) for the first insertion, but relatively high-lying for the second (**TI1′** = 12.1 kcal mol^{-1}; **TI2′** = 7.7 kcal mol^{-1}), a consequence of the additional donor interaction with the Sn center; and (iii) $\mathbf{P_1}$, the first insertion product, is a potential energy well (−5.9 kcal mol^{-1} relative to **R**) and has an activation free energy barrier of 25.9 kcal mol^{-1} relative to **INT**, whereas the activation energy for the second insertion is 30.7 kcal mol^{-1} (**TS2′** − **INT′**). $\mathbf{P_1}$ is therefore anticipated to form quite readily, but the second monomer unit will insert more slowly. Additions of the third and subsequent monomer units (which due to the size of

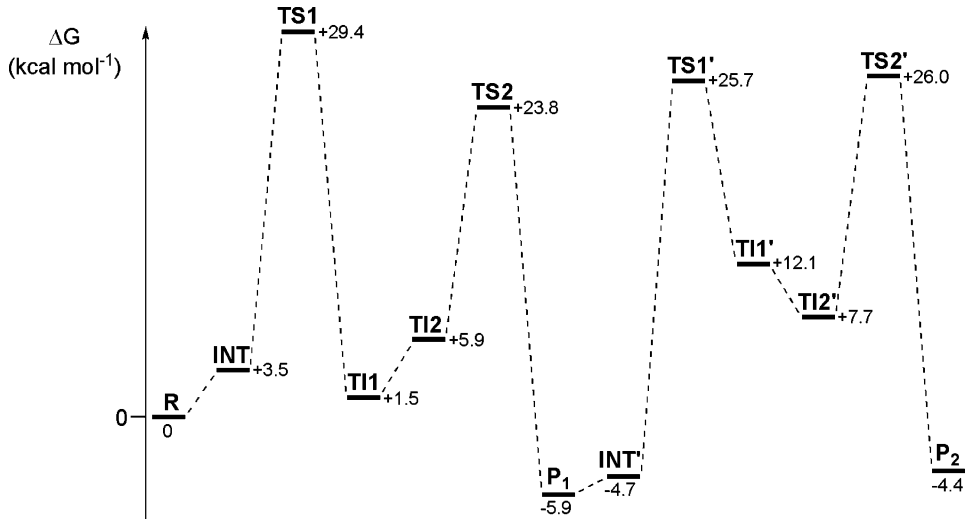

Figure 11. Free-energy changes along the reaction coordinate for insertion of first and second monomer units.

Ⓦ Computational details are available in HTML format, including molecular coordinates (in molfile format), normal mode animations (in XYZ format), together with a Java applet for displaying these, and 3D orbital models (in 3DMF format).

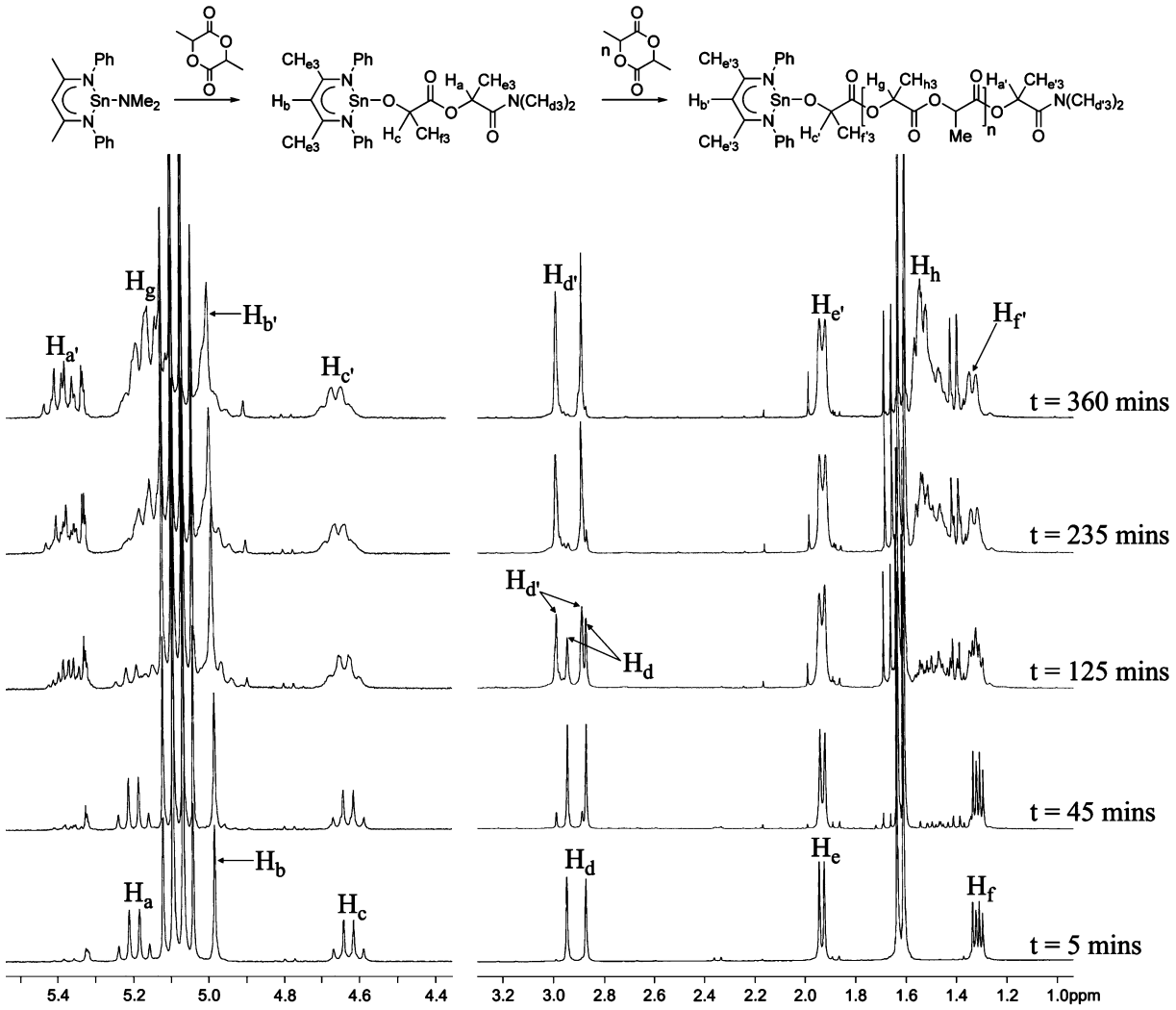

Figure 12. ^{1}H NMR spectra of the reaction between **10** and 5.0 equiv of *rac*-LA (CD_2Cl_2, 250 MHz, 298 K).

the system we have not attempted to model) are expected to be more favorable: as the extruding polymer chain is no longer restricted by interactions with the active site, its entropy should increase with respect to that of the shorter initial chains, thus reducing the activation and reaction free energies for subsequent steps.

Experimental Verification of the Computational Results. To obtain experimental verification of the computational findings, we examined the reaction of the *N*,*N*′-bis(phenyl)-β-diketiminate tin(II) amide complex **10** with 5 equiv of lactide monomer by ^{1}H NMR spectroscopy. **10** was chosen since its ^{1}H NMR spectrum is largely free of resonances in the region 3−6 ppm (where key resonances of propagating species occur) and it displays induction energetics amenable to room-temperature monitoring by NMR spectroscopy. The spectra collected in Figure 12 show that $\mathbf{P_1}$ is formed in essentially quantitative yield within <5 min of mixing **10** with LA at room temperature. The spectrum of $\mathbf{P_1}$ contains two β-diketiminate Me singlet resonances, at δ 1.94 and δ 1.92, a feature shared by complex **14**. $\mathbf{P_1}$ thus clearly lacks a plane of symmetry in solution, which is attributed to the presence of a weak $Sn-O_{carbonyl}$ interaction.

Monitoring the reaction over time shows that $\mathbf{P_1}$ predominates at room temperature for at least 45 min, after which additional resonances become apparent as $\mathbf{P_1}$ is converted into $\mathbf{P_2}$, $\mathbf{P_3}$, etc. For example, the quartets of the methine protons, H_a and H_c, which are observed at δ 5.20 and δ 4.63 in $\mathbf{P_1}$, gradually broaden, with the former (the methine nearest to the amide chain end) shifting to ca. δ 5.4 as further insertions occur and broad polymer methine resonances (H_g) appear between δ 5.1 and δ 5.2. In the same region of the spectrum, the β-diketiminate methine proton (H_b) is initially observed as a sharp singlet at δ 4.98 but, once polymerization commences, gives rise to a broader signal at ca. δ 5.00. For the terminal dimethylamino groups, two sharp singlets are observed, at δ 2.95 and δ 2.87, due to the diastereotopic methyl environments (H_d), a result of the adjacent chiral center, $C(H_a)(CH_{e3})$. These are replaced by two slightly broader downfield resonances ($H_{d'}$) as the oligomerization reaction proceeds. The ^{13}C NMR spectrum of $\mathbf{P_1}$ exhibits two carbonyl resonances, at δ 178.88 and δ 170.04, consistent with the metal lactate resting state.

Discussion

The kinetic studies, along with molecular weight data, clearly show that **2** behaves as a nonaggregated, single-site initiator. This contrasts with tin(II) initiators supported by amidinate ligands,[21,41] for which rate order dependences of 0.2−0.3 have been ascribed to aggregation of metal centers by the propagating ester functionalities. The β-diketiminate ligand presumably

possesses sufficient steric influence to avert such aggregative processes, allowing all of the metal centers to remain continuously active throughout the polymerization. More generally, the (BDI)Sn catalysts show the anticipated trends in polymerization rates with changes to the size of initiating group and the size and electronic properties of the ligand substituents. Thus, the more bulky amide derivatives generally initiate more slowly than their isopropoxide counterparts, and increases in the size of the β-diketiminate aryl substituents or the backbone substituents lead to slower rates of polymerization. Incorporating electron-withdrawing aryl groups accelerates the polymerization, a consequence of the enhanced electrophilicity of the tin centers which will favor monomer binding.

Somewhat to our surprise, the effect of variations to the β-diketiminate ligand on tacticity is minimal, unlike the observations with the analogous zinc system, in which stereoselectivity is dramatically influenced by quite subtle changes to the ancillary ligand substituents.[14] The absence of a significant ligand influence for the tin system suggests that the microstructure of the resultant polylactide is dominated by the tin-centered lone pair, which is known to impose severe constraints on the tin coordination geometry and may give rise to electrostatic repulsions with the lone pairs of the oxygen functionalities of the monomer and propagating chain. Tolman, Hillmyer, and Aubrecht have noted comparable levels of heterotacticity when LA is polymerized using amidinate tin(II) complexes.[21] We have also found that conventional lactide polymerization catalysts, without additional co-ligands, give rise to PLA of similar tacticity.[42] This suggests more generally that divalent tin catalysts are strongly influenced by their stereochemically active metal-based lone pair and that the mechanism is more reasonably described as a *lone-pair-dominated, chain-end-controlled* process, rather than the *ligand-assisted, chain-end-controlled* process found for other (BDI)M systems.

The computational study lends further support to the dominant effect of the tin-based lone pair. A key difference between the computed reaction pathway for the tin system and other (BDI)M initiators is the requirement for a significant initial reorganization of the metal coordination sphere whereby the alkoxide and monomer units first have to interchange sites to allow attack by the alkoxide ligand. This is a direct consequence of the presence of the metal-based lone pair. Furthermore, the calculated geometries of stationary points indicate that minimization of repulsive forces between carbonyl oxygen lone pairs (of either monomer or ring-opened lactate-type structures) and the tin lone pair is a key factor throughout the insertion process, particularly noticeable in the conversion of **INT** into **TS1**, and in the structure of **P**. The extent to which the lone pair dominates the metal coordination sphere can be seen in the computed view of **INT′** shown in Figure 13.

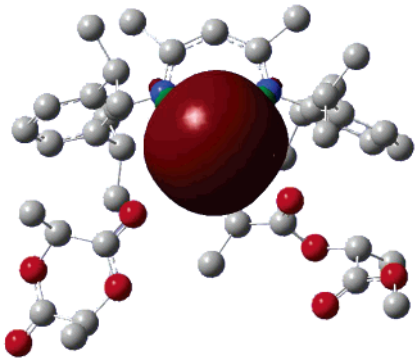

Figure 13. View of **INT′** showing the tin-centered lone pair.

The tin lone pair is also strongly implicated as the cause of the induction period. The calculated free energies for the first two insertion cycles show that, while the first insertion process is exothermic, the subsequent conversion of $\mathbf{P_1}$ into $\mathbf{P_2}$ is far less favorable, an observation verified by NMR spectroscopic studies. It is expected that subsequent insertion steps will become increasingly exothermic as the polymer chain grows, its increased flexibility leading to a favorable entropy term.

Conclusions

In summary, sterically hindered β-diketiminate ligands have been shown to support well-defined, single-site Sn(II) initiators for the polymerization of *rac*-lactide, affording anticipated trends in polymerization rates with variations to the size of the initiating groups and the size and electronic properties of the ligand substituents. Two key differences compared to the polymerization behavior of other metal β-diketiminate initiators are (i) an invariance of the polylactide tacticity across ligands of widely differing steric and electronic properties and (ii) a significant induction period prior to the onset of polymerization. Both of these effects are attributable to the tin-centered lone pair, which not only presents constraints on the tin coordination geometry but also can give rise to electronic repulsions with the lone pairs of the oxygen functionalities in the monomer and in the propagating polymer chain.

Acknowledgment. The Engineering and Physical Sciences Research Council (U.K.) is thanked for financial support (a studentship to A.P.D.).

Supporting Information Available: Full synthetic details and characterization data for complexes **1**−**14**; NOESY and COSY spectra of **14**; crystal data, refinement parameters, and crystallographic information files for **3**, **9**, **12**, and **14** (PDF, CIF). This material is available free of charge via the Internet at http://pub.acs.org.

JA061400A

(41) Nimitsiriwat, N.; Gibson, V. C.; Marshall, E. L.; Elsegood, M. R. J.; Dale, S. H. Manuscript in preparation.

(42) Polylactide samples prepared using $SnOct_2$ and $Sn(NMe_2)_2/^nBuOH$ in toluene at 60 °C have both been found to possess heteroselectivities similar to those observed for the β-diketiminate tin(II) initiators described here: Gibson, V. C.; Marshall, E. L. Unpublished results.